

Review

Recent Advances in the Electroreduction of CO₂ over Heteroatom-Doped Carbon Materials

Ana Cristina Pérez-Sequera , Manuel Antonio Díaz-Pérez  and Juan Carlos Serrano-Ruiz * 

Materials and Sustainability Group, Department of Engineering, Universidad Loyola Andalucía, Avda. de las Universidades s/n, 41704 Dos Hermanas, Seville, Spain; acperez@uloyola.es (A.C.P.-S.); madiaz@uloyola.es (M.A.D.-P.)

* Correspondence: jcserrano@uloyola.es; Tel.: +34-955-641-600 (ext. 2579)

Received: 25 September 2020; Accepted: 13 October 2020; Published: 14 October 2020



Abstract: Ever-growing anthropogenic activity has increased global energy demands, resulting in growing concentrations of greenhouse gases such as CO₂ in the atmosphere. The electroreduction of CO₂ has been proposed as a potential solution for reducing anthropogenic CO₂ emissions. Despite the promising results obtained so far, some limitations hinder large-scale applications, especially those associated with the activity and selectivity of electrocatalysts. A good number of metal catalysts have been studied to overcome this limitation, but the high cost and low earth abundance of some of these materials are important barriers. In this sense, carbon materials doped with heteroatoms such as N, B, S, and F have been proposed as cheaper and widely available alternatives to metal catalysts. This review summarizes the latest advances in the utilization of carbon-doped materials for the electroreduction of CO₂, with a particular emphasis on the synthesis procedures and the electrochemical performance of the resulting materials.

Keywords: CO₂ electroreduction; carbon-doped materials; innovative electrocatalysts; faradaic efficiency; in-situ doping; post-treatment doping

1. Introduction

The ever-growing human population, along with the rapid development of some countries, have resulted in a steady increase of the energy demand. Most of this energy is currently obtained from fossil fuels, the consumption of which releases CO₂ into the atmosphere. As a result, the concentration of CO₂ in the atmosphere increased from ca. 278 ppm before industrialization to ca. 400 ppm in 2018 [1,2]. This increase in CO₂ concentration has been associated with global warming. The average temperature on Earth has been reported to have increased by 1.1 °C since 1880, with the last five years being the warmest period ever recorded [3,4].

In order to mitigate global warming, the scientific community has spurred the search for viable solutions that allow for the reduction of greenhouse gas emissions. The substitution of fossil fuels with renewable sources, such as solar, wind, and hydroelectric sources, has been proposed as a plausible long-term solution. However, renewable sources are usually installed in specific locations (usually far from the demand place) and provide an intermittent supply, which inevitably leads to storage needs [5]. One interesting approach to reducing CO₂ emissions consists of the capture, storage, and subsequent transformation of this molecule into high-value chemical products or fuels [6,7]. This conversion can be carried out by means of photochemical, thermochemical, biochemical, and electrochemical routes. Among these routes, the electrochemical approach is particularly interesting because it can be carried out under significantly milder pressure and temperature conditions (i.e., room temperature and atmospheric pressure) compared to other routes (e.g., catalytic reduction) and without the need for external H₂, since water can be used as the source of both electrons and H⁺ required for the reduction

of CO₂ to organic compounds. In addition, the electroreduction of CO₂ can make use of the surplus of renewable electricity to produce valuable fuels and chemicals [7,8].

Despite these advantages, the electroreduction of CO₂ has important barriers that need to be overcome before the technology is further developed. First, the high potential required to activate the highly stable molecule of CO₂ (as a consequence of the strength of the C=O double bond) represents an important barrier towards efficient conversion. Second, the conversion of CO₂ involves, in some cases, multiple proton and electron transfer reactions. Some of these steps present unfavorable kinetics, which finally results in high overpotentials [9,10]. Third, the parasitic hydrogen evolution reaction (HER), which usually proceeds over the same potential range of the CO₂ electroreduction [11,12], can reduce the faradaic efficiency towards a target product. This undesired process represents an important issue when working with aqueous electrolytes. Fourth, the low solubility of CO₂ in water, combined with inefficient reactor designs, has also been reported to add mass transport limitations to the process [13,14].

One of the most important barriers for the practical applicability of this technology is the reaction complexity. Therefore, the electrochemical reduction of CO₂ usually results in a complex mixture of C₁ and C₂ species (e.g., CO, methane, methanol, formic acid, ethylene, and ethanol, among others). The complexity of this reaction is well-known, since it was first reported by M.E. Royer in the 19th century [15]. Almost a century later, Hori et al. [16–19] still reported the production of a plethora of carbon products, including CO, formic acid, methanol, methane, and ethylene, over several metal catalysts. It is therefore not surprising that efforts over the past years have mostly focused on developing electrocatalysts (i.e., cathodes) able to achieve active, selective, and stable electroreduction of CO₂ into a single target product [20]. With this aim, multiple catalytic materials have been synthesized and tested in this reaction over the last years, including noble (Au, Pt, Ag, and Pd), transition (Ni, Zn, Fe, and Cu), and p-block (Pb, Sn, In, and Bi) metals and combinations of them [21]. As a result of this intense work, it has been concluded that, in aqueous media and under ambient conditions, metals such as Au [22], Ag [23], Zn [24], and Pd [25] are highly selective towards carbon monoxide, while Sn [26], Pb [27], Bi [28], and In [29] generate formic acid as the main product [30–33]. Metals such as Cu have been reported to selectively generate light hydrocarbons ranging from C₁ to C₃ [34–37], while metals such as Pt, Ti, Ni, and Fe have been demonstrated to favor the HER, thereby showing a high selectivity towards H₂ [10].

Apart from the nature of the metal cathode, the configuration of the electrode and the reactor design have both been found to play an important role in the CO₂ electroreduction performance of these materials. For example, the utilization of gas-diffusion metal electrodes instead of full-metal electrodes allowed the faradaic efficiency of Ag and Cu electrodes towards CO and ethylene, respectively, to be increased significantly [38]. The utilization of gas-diffusion electrodes also minimized ohmic losses, thereby allowing current densities relevant for industrial purposes (e.g., 300 mA cm⁻²) to be reached. Diaz-Sainz et al. [39] stressed the importance of the electrode configuration in this reaction by comparing the performance of a large number of electrode configurations and electrocatalysts in this reaction. Gas diffusion and catalyst-coated membrane Bi and Sn electrode configurations provided different results. Therefore, while the coated membrane catalysts achieved higher formate concentrations and reduced energy consumptions, the gas diffusion electrode allowed operations at higher current densities close to 300 mA cm⁻².

Despite the good performance of these metals and the knowledge accumulated in the past years, the high cost and scarcity of some of these materials have spurred the search for cheaper and earth-abundant alternatives [40]. In this sense, carbon-based materials doped with heteroatoms such as N, B, S, and F have received great attention as electrocatalysts owing to their large earth abundance, high surface area, high thermal and mechanical stability, and low cost [19–21]. These materials have been extensively applied for years in fuel-cell-related processes, such as oxygen reduction reactions (ORR) and oxygen evolution reactions (OER), showing outstanding activities comparable to those of conventional Pt-based electrocatalysts [21]. Heteroatom-doped carbon materials present a number of

characteristics (e.g., high stability and strong tolerance to acidic/alkaline aqueous media) that make them particularly attractive for electrocatalytic applications. Additionally, these materials present large versatility in terms of their tailored porous structure and surface chemistry, which can be developed by physical and chemical methods. This is very interesting when it comes to catalytic applications, since the incorporation of surface functionalities can modify the electronic structure of the carbon network and the nature of the active sites. Therefore, the inclusion of heteroatoms with a different electronegativity and size to carbon alters the carbon lattice (i.e., charge density redistribution and structural defects), thereby creating new catalytic sites and inducing new adsorption/activation modes for the CO₂ molecule. This electronic and structural perturbation of the carbon structure has been demonstrated to induce interesting changes in the way that CO₂ interacts with the carbon surface, resulting in an enhanced electroreduction performance [41–45].

The utilization of doped carbon materials as catalysts for the electroreduction of CO₂ has been covered by several reviews in recent years [46–48]. In an excellent review, Wu et al. [46] provided extensive mechanistic information on this reaction over carbon-based materials and identified the main challenges of the process. These authors analyzed the linear scaling relations of metals and discussed how this prevents the binding energies of intermediates from being decoupled on these surfaces, ultimately constraining the reactivity to certain C₁ products (CO vs. CH₄) or increasing the overpotential for the formation of C₂ products. Therefore, the utilization of carbon-doped materials allows the limitation imposed by the classical scaling relation of metals to be overcome and modifies the strength of adsorption of reaction intermediates, resulting in lower overpotentials compared to metal catalysts. These authors discussed the performance of these materials (mostly N-doped) in terms of their ability to generate C₁ or C₂ products. Jia et al. [47] provided an extensive revision of doped carbon materials for this application, although emphasis was mostly placed on transition metal (Fe, Ni, and Co)-doped and other metal-containing carbon materials, while other important dopants, such as S and F, did not receive significant attention. Liu et al. [48] reviewed this topic by using a general approach based on electronic and structural modifications of the carbon lattice upon doping.

The present minireview aims to summarize the most relevant advances made in the utilization of metal-free heteroatom-doped carbon materials for the electroreduction of CO₂. Unlike the reviews cited above, we have employed a different approach (by doping the heteroatom instead of by reaction product) and provided very recent results for other interesting dopants, such as S and F, which were not sufficiently covered in previous works. Instead of using a general approach, we have analyzed the particularities of each dopant (N, B, S, and F) and their effect on the structure of the carbon material. Moreover, we provide additional information on the main techniques used to prepare these materials, which was not the main focus of the above reviews. Therefore, this minireview is focused on two interesting aspects that are inherently connected: the synthesis method and the electrochemical performance of the resulting materials. Finally, our review has a different time frame compared to the above works, being mostly constrained to 2019–2020, with the aim of capturing the rapid development of this area.

2. CO₂ Electroreduction over Heteroatom-Doped Carbon Materials

2.1. Nitrogen-Doped Carbon Materials

2.1.1. Synthesis Methods

Nitrogen has been extensively used as a dopant element for carbon materials [41,43,49]. The covalent radius of nitrogen is very similar to that of carbon (75 vs. 77 pm), which favors its incorporation into the carbon lattice. Nitrogen doping does not result in significant lattice distortions or structural defects of the carbon structure. Instead, due to its higher electronegativity compared to carbon (3.04 vs. 2.55), nitrogen doping mostly induces charge distribution effects, modifying the electronic properties of the original carbon material. A good number of preparation methods have been developed to synthesize nitrogen-doped carbon materials, including in situ (i.e., nitrogen is introduced

during the synthesis of the carbon material) and post-treatment (i.e., nitrogen is added once the carbon material is prepared) doping approaches [43]. With regards to in situ doping, several techniques have been used, including chemical vapor deposition (CVD), pyrolysis, arc charge discharge, laser ablation, and microwave irradiation [49]. CVD is commonly used, since it allows for a controllable catalyst morphology and scalable production, although it is costly and does not allow fine control of the dopant loading. A good range of carbon materials, including graphene [50–55], carbon nanotubes [55–59], microporous carbon [55,60,61], and fullerenes [62], have been doped with nitrogen by in situ techniques. A very simple in situ doping method was recently developed by Sun et al. [63]. These authors fabricated a hierarchical porous N-doped carbon material by simple spray-drying of a solution containing sucrose, urea, and NaCl over the carbon material, followed by pyrolysis at 800 °C and washing to remove NaCl. This cheap and scalable technique resulted in a nitrogen-doped carbon material with an excellent performance as a component of Li-ion batteries and in the electrochemical reduction of CO₂. The particular hierarchical porosity of these materials was described to facilitate electrolyte penetration and electron transfer while providing structural stability. Complex in situ techniques, such as microwave plasma-enhanced CVD, have also been developed to generate novel nitrogen-doped nanodiamonds with an excellent faradaic efficiency (e.g., 90%) towards acetate [64].

Post-treatment doping involves a direct reaction between nitrogen-containing reagents (e.g., urea, ammonia, dicyandiamide, dimethylformamide, amines, etc.) and a pre-synthesized carbon material [49,65]. The reaction is usually carried out at high temperatures for long periods of time, while the carbon material requires a pretreatment to facilitate the incorporation of the doping species. The overall nitrogen content and the nature of the nitrogen functionalities greatly depend on the operation conditions [49,65–67]. Carbon-based materials such as graphene, nanotubes, onion-like carbons, and tubular carbon foams have been successfully doped with nitrogen by post-treatment methods [68,69]. An interesting post-treatment ammonia etching technique was developed by Li et al. [67]. Coal was used as a carbon precursor, resulting in a hierarchical pore carbon structure with highly exposed nitrogen active sites and an excellent CO₂ electroreduction performance (e.g., 90% faradaic efficiency towards CO). Recently, Kuang et al. [70] used Zn-based zeolitic framework-8 (ZIF-8) as a precursor for preparing nitrogen-doped carbon materials. The easy vaporization of ZIF-8 facilitated the doping process during the carbonization step. The resulting carbon material was post-treated with N,N-dimethylformamide (DMF), generating mesoporous nitrogen-doped carbon frameworks with an excellent CO selectivity (92% faradaic efficiency).

2.1.2. CO₂ Electroreduction Performance

Nitrogen doping generates new active sites on the catalyst surface [41]. As shown in Figure 1a, nitrogen atoms can be accommodated on the carbon lattice in several ways, generating different nitrogen functionalities, such as pyridinic, pyrrolic, graphitic, and pyridine-N-oxide (when oxygen functionalities are also present) [41,45,49,65]. These nitrogen functionalities interact differently with the delocalized π electrons provided by the alternate C-C single and double bonds in the graphitic network [43,49] and contribute to the covalent bond with different hybridization (e.g., pyridinic nitrogen presents sp² hybridization and contributes one p-electron per bond to the π system, while pyrrolic N is sp³ hybridized and contributes two p-electrons to the π system). As expected, the catalytic performance of nitrogen-doped carbon materials in the electroreduction of CO₂ greatly depends on the nature of the nitrogen active sites. Several attempts have been made to elucidate the nature of the active species actually involved in the electroreduction process, with no conclusive results having been obtained so far. Recent studies associated the high electroreduction activity of nitrogen-doped carbon materials with the presence of pyridinic functional groups [52–54,58,71–74], whereas others pointed to pyrrolic N [75,76] or even both pyridinic and pyrrolic [51,77] as responsible for the good performance of these materials. Graphitic or quaternary functionalities have also been considered as the main active sites in the electroreduction process [57,62]. Rather than nitrogen functionalities, Wang et al. [78] identified intrinsic carbon defects generated upon nitrogen doping as the actual active sites responsible for CO₂ activation. Therefore, catalysts with low nitrogen loading (Figure 1b,c)

exhibited an optimum CO₂ electroreduction selectivity towards CO, with faradaic efficiencies as high as 95%. Remarkably, un-doped carbon materials also showed excellent faradaic efficiencies towards CO (Figure 1d), thereby revealing that carbon defects play an important role in the electroreduction process. Carbon hybridization was also found to affect the CO₂ electroreduction performance of these materials. Wanninayaque et al. [79] prepared several nitrogen-doped materials containing both diamond (sp³) and graphitic (sp²) carbon structures. These authors concluded that the carbon structure hosting the nitrogen dopant was relevant in determining the electrocatalytic performance of the material. Therefore, those materials with higher sp²/sp³ ratios displayed an excellent CO₂ electroreduction performance (80% faradaic efficiency to CO), while those containing high sp³ carbon contents catalyzed the parasitic HER.

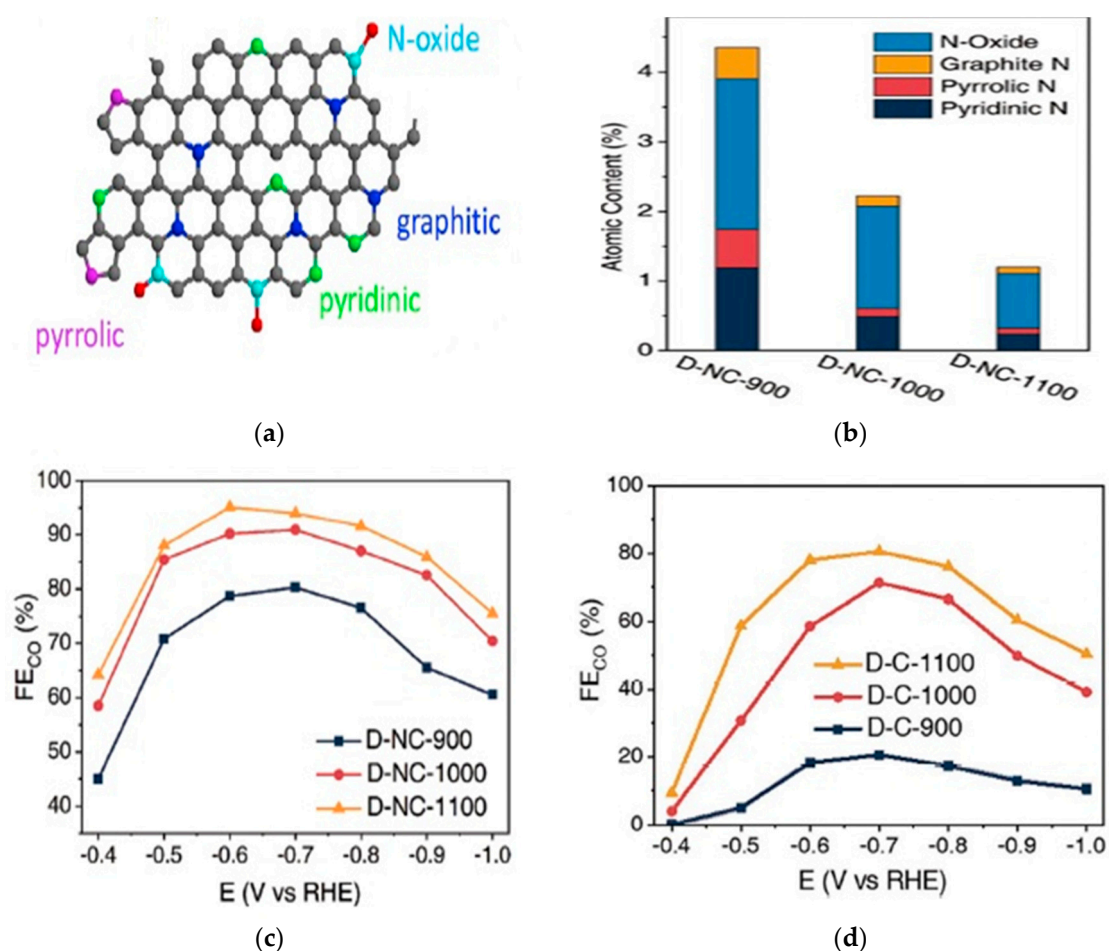


Figure 1. (a) Nitrogen atom configuration in a graphene network, reproduced from [80], Copyright (2020), with permission from Elsevier; (b) N content of doped material D-NC-1100; (c) Faradaic efficiency to CO (FE_{CO}) versus applied potential of the N-doped catalysts; (d) FE_{CO} versus the applied potential of the un-doped catalyst, reproduced from [78], Copyright (2020), with permission from John Wiley and Sons.

Nitrogen-doped carbon electrocatalysts also exhibited outstanding stabilities [58,71,81]. As shown in Figure 2a, nitrogen-doped nanotubes maintained the current density (6 mA/cm²) and faradaic efficiencies to CO at around 90% for 60 h of operation [57]. Zhu et al. [82] developed 1D/2D nitrogen-doped carbon nanorod arrays/nanosheets, with the selectivity, current density, and structural stability being maintained for more than 30 h of continuous operation (Figure 2b).

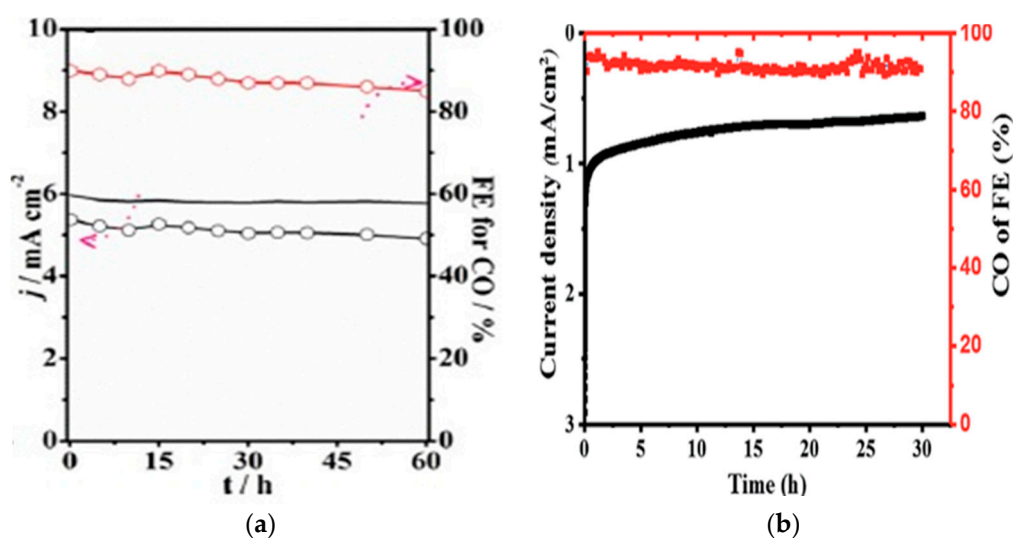


Figure 2. (a) Stability test (total current density, faradaic efficiency, and current density for CO production) of nitrogen-doped carbon nanotubes at -0.9 V vs. a reversed hydrogen electrode (RHE), reproduced from [57], Copyright (2020), with permission from John Wiley and Sons. (b) Stability test on a 1D/2D nanorod array/nanosheets-900 electrode at -0.45 V in CO_2 -saturated 0.5 M KHCO_3 , reproduced from [82], Copyright (2020), with permission from the Royal Society of Chemistry.

Co-doping nitrogen with other elements such as P resulted in carbon materials with an outstanding electroreduction performance. Chen et al. [83] synthesized, for the first time, a nitrogen, phosphorous co-doped carbon aerogel with an improved CO_2 electroreduction performance (99% faradaic efficiency to CO) at partial current densities of $143.6 \text{ mA}\cdot\text{cm}^{-2}$ (one of the highest values reported for this reaction). This co-doped carbon material showed a large electrochemical active area and high electronic conductivity while suppressing the HER.

2.2. Boron-Doped Carbon Materials

2.2.1. Synthesis Methods

The affinity between carbon and boron has been used to improve the activity and stability of carbon materials in electrocatalytic applications. The promotional effect of boron in carbon materials has not yet been well-elucidated, although an electronic effect (rather than structural distortion or the generation of defects) is usually invoked in the literature. Some studies suggest that boron doping allows the electronic properties of carbonaceous materials to be modified, given the different electronegativity of the two atoms (2.04 and 2.55 for boron and carbon, respectively) [41]. Boron doping is believed to induce charge polarization in the carbon framework, thereby allowing the stabilization of important reaction intermediates generated during the electroreduction process. Furthermore, boron doping is believed to decrease the energy barriers for CO_2 electroreduction by stabilizing the negatively polarized O atoms of the CO_2 molecule, facilitating its chemisorption on the carbon material [41,42,45]. Nevertheless, additional studies are required to fully understand the positive effect of boron doping on carbon materials.

As in the case of nitrogen-doped materials, CVD is the most common in situ doping method, either alone [66] or in combination with microwave plasma (MPCVD) [70–73]. CVD has been used to synthesize boron-doped diamonds (BDD) with a high selectivity towards formic acid [84–86] and methanol [87]. Liu et al. [88] used a hot filament vapor deposition technique to obtain boron and nitrogen co-doped diamonds (BND). These BND were found to be highly selective in electroreducing CO_2 to C_2 products (e.g., ethanol, 93% faradaic efficiency). Apart from CVD, other in situ methods allow the accommodation of boron atoms in carbon structures. Jia et al. [89] synthesized nitrogen and boron co-doped porous carbon (NBPC) by using an interesting salt-sugar methodology. A sodium

chloride-glucose solution was used as a carbon source, with ammonia chloride and boron acid serving as nitrogen and boron precursors, respectively. These precursors were mixed in a solution, which was freeze-dried under vacuum to maintain a highly homogeneous mixed state and structure. The resulting solid was pyrolyzed at 600 and 900 °C under argon and washed with deionized water to remove impurities. The as-obtained NBPC catalyst displayed a high level of activity and faradaic efficiency (83%) towards CO during the electroreduction of CO₂. Post-treatment boron doping has been used to a significant lower extent compared to in situ doping. In these methods, boron doping is achieved by treating pristine carbon materials with boron precursors at high temperatures [66]. One of the few examples of this methodology was developed by Skreekanth et al. [90]. These authors synthesized boron-doped graphene by heating a uniform mixture of graphene oxide and boric acid at 900 °C under an argon atmosphere. The as-obtained material exhibited a good electroreduction performance, with formate being produced with a faradaic efficiency of 66%. Boron-doped carbon materials (mostly BDD) have also been used as supports of metals in the electroreduction of CO₂. These metals are usually deposited by electrodeposition via chronoamperometric techniques [91–100].

2.2.2. CO₂ Electroreduction Performance

Recent efforts on the boron doping of carbonaceous materials have focused on the production of BDD [87,101,102]. BDD show excellent electrochemical properties and an outstanding mechanical stability and corrosion resistance, making them promising materials for CO₂ electroreduction purposes. In these materials, boron atoms substitute sp³ carbon atoms in the diamond structure, providing electronic conductivity to the otherwise insulator material. Moreover, BDD are superior in terms of their potential window, background current, chemical inertness, and mechanical durability compared with conventional electrodes. Their wide potential window is particularly relevant in that it allows the electroreduction process to be conducted at voltages well-separated from that of the HER, thereby avoiding a parasitic reaction. The electrochemical performance of BDD electrodes depends on factors such as the presence or absence of sp² carbon impurities, surface termination, boron loading, and the nature of the electrolyte [103,104]. These factors have recently been studied by Xu et al. [103]. These authors synthesized BDD with several doping loadings (0.01–2%) and used them as cathodes in the electrochemical reduction of CO₂. Formic acid was the main product in all cases, with the highest faradaic efficiency being obtained at a 0.1% boron content. Higher boron loadings resulted in the selectivity mostly shifting to H₂ (via HER) and CO (Figure 3a). These results were explained by changes in adsorbability and tensile stress induced by boron doping on the diamond structure. The electrolyte was found to be an important factor in determining the product selectivity of BDD materials [84,87]. Tomisaki et al. [104] found a correlation between the product selectivity and the electrolyte during the electroreduction of CO₂ over BDD. Therefore, the utilization of KClO₄ as a catholyte mostly generated CO and formic acid, while aqueous KCl almost exclusively produced formic acid (Figure 3b). CO₂^{•−} intermediates being preferentially adsorbed on BDD in aqueous KClO₄ were invoked to explain these results. The presence of these anionic intermediates was followed by attenuated total reflectance-infrared spectroscopy (ATR-IR).

The long-term stability of BDD materials was investigated by Ikemiya et al. [85]. These authors developed a smart solution to ensure the continuous production of formic acid for long periods of time. Two BDD electrodes (BDD 1 and BDD 2) were used alternatively as an anode and cathode by reversing the polarity of the cell every 24 h. Upon polarity reversal, the spent BDD was almost fully regenerated by electrochemical oxidation in an SO₄^{2−}-containing electrolyte, while the second BDD electrode operated as a cathode and continued with the production of formic acid (Figure 4). Formic acid production rates as high as 328 μmol·h^{−1}·cm^{−2} were obtained at a current density of −20 mA·cm^{−2}. These rates were claimed to be the highest ever obtained over plate electrodes, revealing the industrial applicability of this double BDD electrode approach.

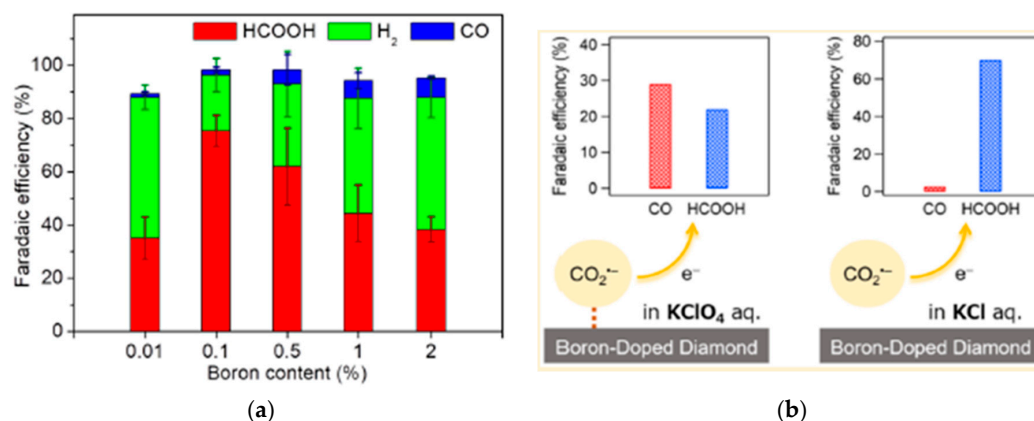


Figure 3. (a) Faradaic efficiencies to formic acid, hydrogen, and carbon monoxide on boron-doped diamond (BDD) electrodes with various boron contents, reproduced from [103], Copyright (2020), with permission from Elsevier. (b) Effect of the catholyte on the product selectivity and faradaic efficiency of BDD, reproduced from [104], Copyright (2020), with permission from the American Chemical Society.

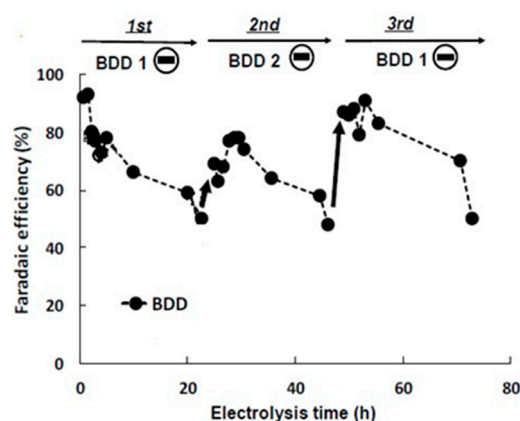


Figure 4. Long-term test on a double BDD cell. The faradaic efficiency changes upon alternating the polarity of the BDD electrodes, reproduced from [85], Copyright (2020), with permission from the American Chemical Society.

This pioneer work has motivated other researchers to further explore this double BDD electrode approach. Lou et al. [105] reported a BDD-BDD system for the simultaneous conversion of CO_2 and wastewater purification. CO_2 was mostly converted to formaldehyde on the BDD cathodic chamber, while organic wastes were decomposed by oxidation over the BDD anode. Potassium hydrogen phthalate (KHP) was used as an organic waste. This process showed a high faradaic efficiency to formaldehyde, while allowing the removal of organic waste on the anode (Figure 5). This work is interesting in that it suggests that the electrochemical reduction of CO_2 can be effectively coupled with wastewater purification to simultaneously generate high-value chemical products and clean water.

Co-doping boron with other heteroatoms has been demonstrated to produce beneficial effects in the electroreduction of CO_2 [88,89,106]. Mou et al. [107] used boron phosphide nanoparticles to perform the electrochemical reduction of CO_2 to methanol with a high selectivity (faradaic efficiency of 92%). Density functional theory (DFT) calculations revealed that boron and phosphorous can synergistically promote the binding and activation of the CO_2 molecule. Therefore, this study paves the way for using boron and phosphorus co-doped carbon materials in the electroreduction of CO_2 .

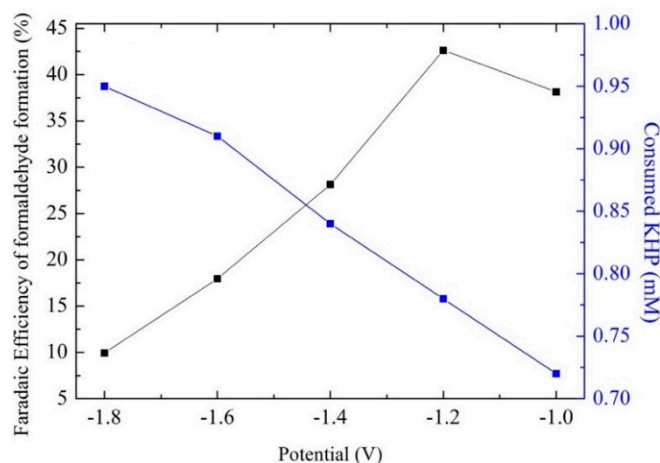


Figure 5. Faradaic efficiency to formaldehyde (black) and potassium hydrogen phthalate (KHP) consumption (blue) as a function of the potential in a BDD-BDD cell, reproduced from [105], Copyright (2020), with permission from Elsevier.

2.3. Sulfur-Doped Carbon Materials

2.3.1. Synthesis Methods

Unlike nitrogen and boron, sulfur doping does not generate significant charge redistributions in the carbon structure, since the electronegativity of this element is very similar to that of carbon (2.58 vs. 2.55) [43]. Instead, the accommodation of sulfur in the carbon structure induces significant structural defects, given the large size of this element (105 pm). These structural defects increase the specific surface area of the material and expose new active sites, increasing the activity of the catalyst [108]. Furthermore, due to its larger atomic size and greater polarizability compared with carbon, sulfur doping provides a high spin density, edge strain, and charge delocalization characteristics to the carbon structure [41]. Sulfur-doped carbon materials are commonly prepared by CVD, plasma treatment, and thiourea-etching methods [108]. In recent years, less complex preparation methods involving the simple pyrolysis of a mixture of sulfur and carbon precursors have been developed. Li et al. [109] described a new technique for preparing sulfur-doped and sulfur, nitrogen-co-doped polymer-derived carbons with a large surface area and well-developed microporosity. Poly (4-styrenesulfonic acid-co-maleic acid) sodium was used as a sulfur and carbon precursor, while urea served as a nitrogen-containing reagent. These precursors were mixed, pyrolyzed at 800 °C under nitrogen, and finally washed with water to remove the sodium ions. When used as cathodes, these materials released CO and CH₄ with modest faradaic efficiencies. Pan et al. [110] reported a simple method for preparing nitrogen and sulfur co-doped carbon layers by layer-structured carbon nitride-templated pyrolysis. Citric acid (as a carbon precursor) and thiourea (a sulfur- and nitrogen-containing reagent) were mixed and pyrolyzed under argon at varying temperatures (800–1000 °C). The catalyst prepared at 900 °C showed higher faradaic efficiencies to CO (92%) and lower overpotentials (490 mV) than its sulfur-free counterpart, revealing a beneficial effect of sulfur-doping.

2.3.2. CO₂ Electroreduction Performance

When it comes to CO₂ electroreduction, the sulfur-doping of carbon materials is normally carried out in combination with other heteroatoms (e.g., nitrogen). A recent breakthrough was reported by Yang et al. [111]. These authors developed a simple in-situ route involving the electrospinning of polymer nanofibers and subsequent carbonization to synthesize nitrogen and sulfur co-doped hierarchically porous carbon nanofibers. When used as cathodes, these materials exhibited an outstanding faradaic efficiency of 94% towards CO at a high current density of $-103 \text{ mA}\cdot\text{cm}^{-2}$. The materials remained stable after 36 h of electrolysis, as revealed by energy-dispersive x-ray

spectroscopy (EDX). Pyridinic groups and carbon-bonded sulfur atoms were suggested to be the active sites in the electroreduction process. DFT revealed that these sites reduced the energy barrier for the binding of $^*\text{COOH}$ intermediates compared to nitrogen-doped materials (Figure 6a). These intermediates play a key role in the formation of CO. Similar results (93% faradaic efficiency to CO) at lower current densities ($-5.2 \text{ mA}\cdot\text{cm}^{-2}$) were obtained by Li et al. [112] over nitrogen and sulfur co-doped hollow carbon nanospheres. The addition of sulfur was suggested to increase the number of active sites of the material. In addition, DFT revealed lower energy barriers for the formation of $^*\text{COOH}$ intermediates on pyridinic sites adjacent to carbon atoms bonded to sulfur compared to regular pyridinic sites (Figure 6b). A significant electron spin density redistribution upon sulfur doping was also invoked to explain the superior performance of the co-doped material compared to its nitrogen-doped counterpart. The cathode displayed a stable performance for 20 h of continuous operation.

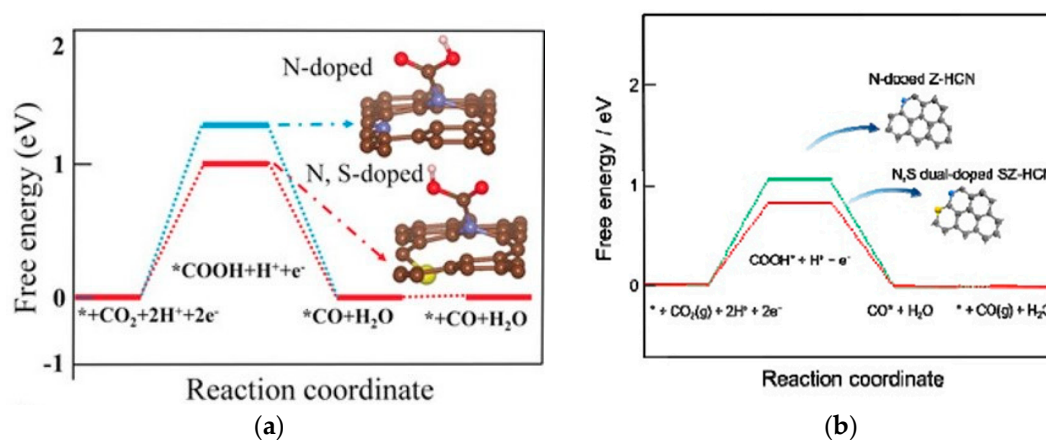


Figure 6. (a) Free energy diagram of CO₂ electrochemical reduction to CO on nitrogen-doped graphene and nitrogen, sulfur co-doped grapheme, reproduced from [111], Copyright (2020), with permission from John Wiley and Sons. (b) Free energy diagram of CO₂ reduction to CO on nitrogen-doped carbon hollow carbon nanospheres and nitrogen, sulfur co-doped hollow carbon nanospheres, reproduced from [112], Copyright (2020), with permission from Elsevier.

Han et al. [113] prepared nitrogen and sulfur co-doped carbon nanoweb structures and used them as cathodes for the electroreduction of CO₂. To study the effect of sulfur doping on the electroreduction performance of these materials, several carbon nanowebs with varying sulfur loadings were prepared. Two different sulfur functional groups (i.e., thiophene-like and oxidized sulfur) were identified and quantified by X-ray photoelectron spectroscopy (XPS). As shown in Figure 7, there was a clear correlation between the thiophene-like sulfur/oxidized sulfur ratio of the nanoweb materials and their selectivity to CO. Both the efficient exposure of active sites upon sulfur doping and the modification of the electronic properties of pyridinic sites (by thiophene-like sulfur atoms with a lone pair of electrons) were invoked to explain this behavior. The performance of the materials remained stable for 20 h of continuous operation.

Wang et al. [114] synthesized nitrogen and sulfur co-doped carbon nanosheets with a high (85%) and stable (for 20 h) faradaic efficiency towards CO. This excellent performance was ascribed to the highly porous 2D unique structure of these materials, along with a synergistic effect of sulfur and nitrogen in the carbon structure. In this sense, the presence of sulfur was found to increase both the porosity and number of exposed active sites of the carbon material.

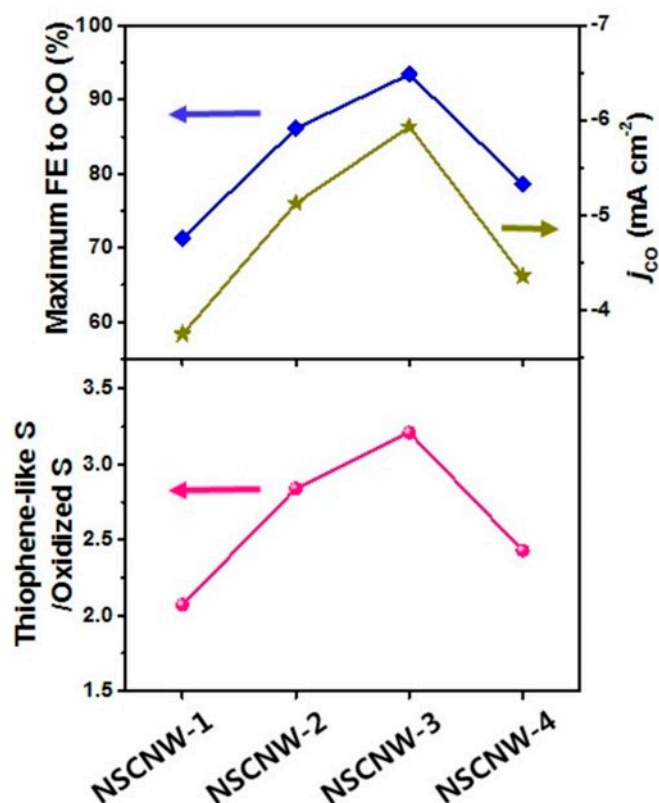


Figure 7. Correlation of the thiophene-like sulfur to oxidized sulfur ratio with the faradaic efficiencies to CO and current densities for several nitrogen and sulfur co-doped carbon nanoweb cathodes tested in the electroreduction of CO₂, reproduced from [113], Copyright (2020), with permission from John Wiley and Sons.

2.4. Fluorine-Doped Carbon Materials

2.4.1. Synthesis Methods

Owing to its low size (57 pm) and high electronegativity (4.0), the fluorine doping of carbon materials typically results in the formation of new strong C-F covalent bonds, rather than the substitution of carbon atoms in the lattice. These newly formed C-F covalent bonds are strongly polarized (i.e., they have a partially ionic character), with the electron density being concentrated around the fluorine atom and the carbon atom bearing a positive partial charge. These positively charged carbon atoms have been proposed to act as active sites in the electroreduction of CO₂ [45]. Pyrolysis has been commonly used to prepare fluorine-doped carbon materials [110,111]. Xie et al. [115] synthesized interlayer fluorine-doped carbon by the simple pyrolysis of a commercial carbon mixed with polytetrafluoroethylene (PTFE, the fluorine source) at 950 °C under argon. Fluorine doping was found to induce structural defects in the carbon lattice, while XPS revealed the presence of CF and CF₂ functional groups (Figure 8a). Unlike the pristine carbon material, the fluorinated cathode exhibited an excellent selectivity towards CO and significant suppression of the HER at voltages ranging from −0.5 to −0.7 V (Figure 8b). Positively charged carbon atoms generated upon interaction with fluorine were suggested to strongly adsorb *COOH intermediates, leading to preferential CO production and HER suppression.

Wang et al. [116] prepared fluorine-doped cage-like porous carbons by using a structure-directing agent such as tetraethyl orthosilicate (TEOS), resorcinol and formaldehyde as carbon precursors, and PTFE as a fluorine source. Once precipitated, the solid was pyrolyzed at 900 °C under argon and subsequently treated with HF to remove SiO₂. The as-obtained solid was finally treated with CO₂ to create open pores on the carbon shell. Similar procedures were reported to prepare fluorine-doped carbon sphere, fluorine-doped hollow carbon sphere, and fluorine-doped commercial

carbon materials. These materials displayed a large surface area, abundant micropores, and a high electrical conductivity. Among these materials, the fluorine-doped cage-like porous carbons exhibited the optimum performance in the electroreduction process, with faradaic efficiencies towards CO close to 90% at a current density as high as $37.5 \text{ mA}\cdot\text{cm}^{-2}$. The catalyst maintained more than 97% of its initial current density and faradaic efficiency to CO after 12 h of electrolysis. XPS revealed the existence of semi-ionic C-F bonds (i.e., F- sp^2 C) in the carbon structure. These highly polarized carbon atoms, along with the edge sites of each circular opening pore at the carbon shell, were suggested to be highly effective in decreasing the energy barrier for CO_2 activation. Panomsuwan et al. [117] in situ synthesized fluorine-doped carbon nanoparticles by a simple one-step solution plasma method with a mixture of toluene and trifluorotoluene. Although these materials were employed in a different electrochemical application (the oxygen reduction reaction, ORR), the simplicity and mild conditions of the synthesis process (e.g., near ambient temperature and atmospheric pressure) hold great promise for preparing CO_2 electroreduction cathodes.

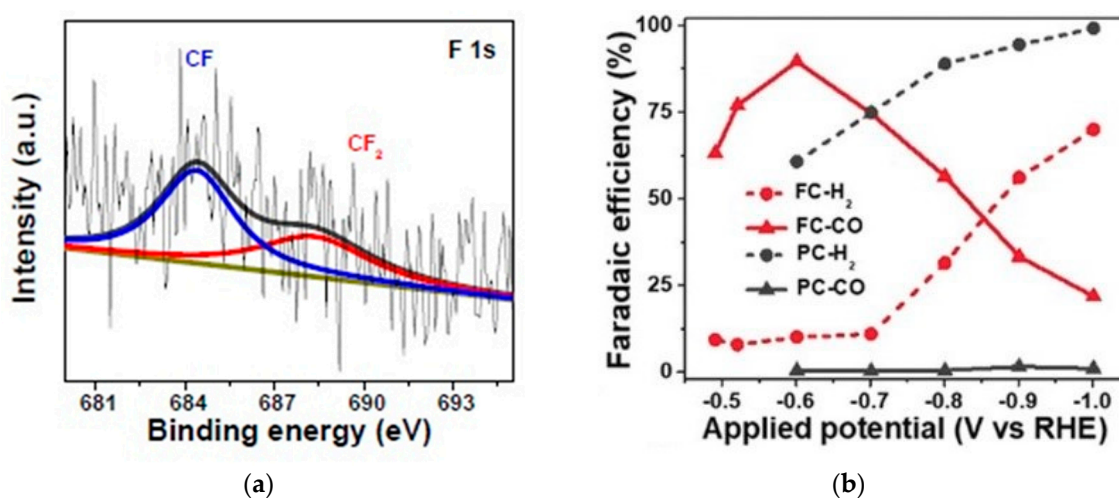


Figure 8. (a) High-resolution X-ray photoelectron spectroscopy (XPS) spectrum of F 1s for the FC catalyst. (b) Faradaic efficiency to CO and H₂ as a function of the applied potential on FC compared with PC (pristine carbon), reproduced from [115], Copyright (2020), with permission from John Wiley and Sons.

With regard to post-treatment techniques, a number of interesting materials have been synthesized, although their performance in the electroreduction of CO_2 remains unexplored. Zaderko et al. [118] prepared fluorine-containing carbon microspheres with a high thermal and chemical stability. The carbon microspheres, pre-synthesized with fructose and citric acid, were subsequently treated under argon with fluorine-containing reagents such as dichlorodifluoromethane, 1,1,1,2-tetrafluoroethane, and PTFE at temperatures of 500, 490, and 665 °C, respectively. Pu et al. [119] developed a simple method for functionalizing graphene oxide (GO) with fluorine. Therefore, fluorinated graphene oxide (FGO) was obtained by exposing pre-synthesized GO to gaseous HF at low temperatures (e.g., 50–130 °C).

2.4.2. CO_2 Electroreduction Performance

Like sulfur, fluorine has also been used as a promoter to improve the performance of nitrogen-doped materials in the electroreduction of CO_2 . Perhaps the most relevant example of this approach is the one reported by Wang et al. [120]. These authors prepared a perfluorinated covalent triazine carbon framework that presented an outstanding selectivity to methane (faradaic efficiency close to 100%). Fluorine modified the intrinsic tendency of nitrogen sites to generate CO by favoring a new reaction pathway towards methane, as revealed by a meticulous DFT analysis. Pan et al. [121] also improved the performance of nitrogen-doped carbon materials by fluorine doping. Therefore, nitrogen and

fluorine co-doped holey carbon layers showed faradaic efficiencies to CO as high as 90% at a low overpotential of 490 mV, while the nitrogen-doped counterpart exhibited modest faradaic efficiencies (60%) at significantly higher overpotentials (800 mV). In addition, the nitrogen and fluorine co-doped material showed outstanding current and faradaic efficiency stabilities for 40 h of continuous operation. DFT revealed that fluorine atoms changed the catalytic behavior of pyridinic nitrogen atoms by altering the charge density on these sites.

3. Conclusions

In the last few years, metal-free materials such as carbon materials doped with heteroatoms have gained significant attention due to their promising performance in a number of electrochemical processes, including the electrochemical reduction of CO₂. Herein, we provide an overview of recent (published within the last two years) works using carbon materials doped with heteroatoms (e.g., N, B, S, and F) for this relevant process, with a particular emphasis on the synthesis procedure (in situ and post-treatment) and electrochemical performance (mostly the faradaic efficiency and current density). Nitrogen-doped carbon materials were found to enhance the electrochemical performance of the cathode by providing new functional groups (e.g., pyridinic, pyrrolic, graphitic, and pyridine-N-oxide functionalities) in the carbon network. In these materials, efforts are mostly focused on (i) elucidating the role of each nitrogen functionality in the electroreduction process and (ii) developing synthesis routes able to generate these functionalities in a controllable fashion. Boron doping has mostly been applied to diamonds (BDD), which have attracted great attention due to their high durability and electrochemical stability. The robustness of these materials has been exploited to develop double BDD approaches for the long-term continuous production of valuable chemicals (e.g., formic acid and formaldehyde), in combination with environmentally relevant processes, such as the oxidation of water contaminants. Sulfur has been extensively used as a co-dopant agent to improve the catalytic behavior of nitrogen-doped carbon materials. Therefore, sulfur and nitrogen co-doped carbon materials have shown high faradaic efficiencies to CO as a result of a synergetic effect of both heteroatoms and the ability of sulfur to modify the electronic properties of nitrogen functionalities. Finally, the high electronegativity of fluorine has been exploited to significantly modify the charge density of carbon atoms in a wide range of carbon structures. Therefore, by forming different types of C-F bonds (i.e., covalent and semi-ionic) and by inducing a partial positive charge density on the carbon atom, fluorine-doped carbon materials have provided high electroreduction activities and outstanding faradaic efficiencies to CO and methane.

Despite these promising results, some aspects should be improved and better understood before these materials can be considered for large-scale CO₂ electroreduction applications. For example, the effectiveness, simplicity, and cost of some of the doping techniques described herein should be significantly improved before envisaging mass production. Simple and inexpensive doping techniques allowing uniform heteroatom doping and fine control over the functional groups inserted into the carbon material are still necessary. This last aspect is crucial for gaining insights into the synthesis–structure relationship of these complex materials. The selection of appropriate carbon materials allowing a uniform distribution of the doping atoms is required to develop electrocatalysts with a good performance. Moreover, the development of techniques able to identify the actual active sites on the electrocatalysts may contribute to elucidating the specific reaction mechanism operating on each catalyst, as well as to improving the doping techniques.

The proper size of the nitrogen atom (very similar to that of carbon) has facilitated and spurred the production and development of a large number of nitrogen-doped carbon materials in the last decade. However, this easy accommodation of the nitrogen atom on the carbon structure is also a source of complexity, since nitrogen can be present in many different places in the carbon network, generating different functionalities with different reactivities/interactions towards the CO₂ molecule. Therefore, it is particularly important for nitrogen-doped carbon materials to develop synthesis methods allowing fine control over the fate of nitrogen atoms in the carbon structure. Simultaneously, the development of

new in situ operando spectroscopic techniques such as Raman and diffuse reflectance infrared Fourier transform spectroscopy (DRIFT) can help gain insights into the specific reactions taking place over each of the nitrogen functionalities, while new DFT studies can shed light on the role of these functionalities in changing the reaction pathways so that the synthesis can be directed to products other than CO. In the case of boron-doped carbon materials, it is necessary develop knowledge on the origin of the actual beneficial effect of boron in the electroreduction of CO₂ (i.e., electronic or structural modifications of the carbon lattice). Moreover, boron-doping has mostly focused on robust and stable diamonds, while the doping of other interesting carbon allotropes remains unexplored. The sulfur-doping of carbon materials has been significantly less exploited than nitrogen and boron, mostly because the large size of the atom hinders accommodation in the carbon network. While the combination of sulfur and nitrogen is well-known, the use of sulfur with other dopants remains largely unexplored and could be worth testing. Finally, the high electronegativity and small size of fluorine provide opportunities to significantly modify the electronic distributions of carbon structures by forming new highly polarized C-F bonds. However, the role of these new functionalities in the CO₂ electroreduction process is not yet fully understood and significant research is needed to elucidate the actual role of these new sites. Furthermore, new preparation methodologies should be developed to allow safer and cleaner handling of this hazardous element.

Author Contributions: All authors contributed equally to this work. All authors have read and agreed to the published version of the manuscript.

Funding: J.C.S.R. would like to thank the Spanish Ministry of Science and Innovation for financial support through the Ramón y Cajal Program, Grant: RYC-2015-19230 and the Research, Development and Innovation projects program, Project number: PID2019-108453GB-C22. J.C.S.R. would also like to thank Junta de Andalucía for financial support through the projects PY18-RE-0012 and IE18_0047_FUNDACIÓN LOYOLA.

Conflicts of Interest: The authors declare no conflict of interest.

References

1. WMO (World Meteorological Organization). *WMO Greenhouse Gas Bulletin. The State of Greenhouse Gases in the Atmosphere Based on Global Observations through 2018*; WMO: Geneva, Switzerland, 2019.
2. Petroleum British. *BP Statistical Review of World Energy*; Petroleum British: London, UK, 2019.
3. WMO (World Meteorological Organization). *The Global Climate 2015–2019*; WMO: Geneva, Switzerland, 2019.
4. Hoegh-Guldberg, O.; Jacob, M.D.; Taylor, M.; Bindi, S.; Brown, I.; Camilloni, A.; Diedhiou, R.; Djalante, K.L.; Ebi, F.; Engelbrecht, J.; et al. Impacts of 1.5 °C of Global Warming on Natural and Human Systems. In *Global Warming of 1.5 °C: An IPCC Special Report on the Impacts of Global Warming of 1.5 °C above Pre-Industrial Levels and Related Global Greenhouse Gas Emission Pathways, in the Context of Strengthening the Global Response to the Threat of Climate Change*; V. Masson-Delmotte: Geneva, Switzerland, 2018; pp. 175–311.
5. Abdmouleh, Z.; Gastli, A.; Ben-Brahim, L.; Haouari, M.; Al-Emadi, N.A. Review of optimization techniques applied for the integration of distributed generation from renewable energy sources. *Renew. Energy* **2017**, *113*, 266–280. [[CrossRef](#)]
6. Li, L.; Wong-Ng, W.; Huang, K.; Cook, L.P. *Materials and Processes for CO₂ Capture, Conversion, and Sequestration*, 1st ed.; The American Ceramic Society, Wiley: Hoboken, NJ, USA, 2018; ISBN 9781119231066.
7. Chen, C.; Kotyk, J.F.K.; Sheehan, S.W. Progress toward Commercial Application of Electrochemical Carbon Dioxide Reduction. *Chem* **2018**, *4*, 2571–2586. [[CrossRef](#)]
8. Jung, Y. On the Selective Heterogeneous CO₂ Electroreduction to Methanol. *ACS Catal.* **2015**, *5*, 965–971. [[CrossRef](#)]
9. Zhou, Z.Y.; Sun, S.G. A breakthrough in electrocatalysis of CO₂ conversion. *Natl. Sci. Rev.* **2017**, *4*, 155–156. [[CrossRef](#)]
10. Gao, D.; Cai, F.; Wang, G.; Bao, X. Nanostructured heterogeneous catalysts for electrochemical reduction of CO₂. *Curr. Opin. Green Sustain. Chem.* **2017**, *3*, 39–44. [[CrossRef](#)]
11. Hashiba, H.; Weng, L.C.; Chen, Y.; Sato, H.K.; Yotsuhashi, S.; Xiang, C.; Weber, A.Z. Effects of electrolyte buffer capacity on surface reactant species and the reaction rate of CO₂ in Electrochemical CO₂ reduction. *J. Phys. Chem. C* **2018**, *122*, 3719–3726. [[CrossRef](#)]

12. Pupo, M.M.d.P.; Kortlever, R. Electrolyte Effects on the Electrochemical Reduction of CO₂. *ChemPhysChem* **2019**, *20*, 2926–2935. [[CrossRef](#)] [[PubMed](#)]
13. Higgins, D.; Hahn, C.; Xiang, C.; Jaramillo, T.F.; Weber, A.Z. Gas-Diffusion Electrodes for Carbon Dioxide Reduction: A New Paradigm. *ACS Energy Lett.* **2019**, *4*, 317–324. [[CrossRef](#)]
14. Weng, L.C.; Bell, A.T.; Weber, A.Z. Modeling gas-diffusion electrodes for CO₂ reduction. *Phys. Chem. Chem. Phys.* **2018**, *20*, 16973–16984. [[CrossRef](#)] [[PubMed](#)]
15. Royer, M. Réduction de l'acide carbonique en acide formique. *Compt. Rend.* **1870**, *70*, 731–732.
16. Hori, Y.; Suzuki, S. Electrolytic Reduction of Carbon Dioxide at Mercury Electrode in Aqueous Solution. *Bull. Chem. Soc. Jpn.* **1982**, *55*, 660–665. [[CrossRef](#)]
17. Hori, Y.; Suzuki, S. Cathodic Reduction of Carbon Dioxide for Energy Storage. *J. Res. Inst. Catal. Hokkaido Univ.* **1983**, *30*, 81–82.
18. Hori, Y.; Kikuchi, K.; Suzuki, S. Production of CO and CH₄ in Electrochemical Reduction of CO₂ at metal electrodes in aqueous Hydrogen Carbonate Solution. *Chem. Lett.* **1985**, *14*, 1695–1698. [[CrossRef](#)]
19. Hori, Y.; Kikuchi, K.; Murata, A.; Suzuki, S. Production of Methane and Ethylene in Electrochemical Reduction of Carbon Dioxide At Copper Electrode in Aqueous Hydrogencarbonate Solution. *Chem. Lett.* **1986**, *15*, 897–898. [[CrossRef](#)]
20. She, Z.W.; Kibsgaard, J.; Dickens, C.F.; Chorkendorff, I.; Nørskov, J.K.; Jaramillo, T.F. Combining theory and experiment in electrocatalysis: Insights into materials design. *Science* **2017**, *355*, eaad4998.
21. Qiao, J.; Liu, Y.; Hong, F.; Zhang, J. A Review of Catalysts for the Electroreduction of Carbon Dioxide to Produce Low-Carbon Fuels. *Chem. Soc. Rev.* **2014**, *43*, 8190600893. [[CrossRef](#)]
22. Hossain, M.N.; Liu, Z.; Wen, J.; Chen, A. Enhanced catalytic activity of nanoporous Au for the efficient electrochemical reduction of carbon dioxide. *Appl. Catal. B Environ.* **2018**, *236*, 483–489. [[CrossRef](#)]
23. Fan, T.; Wu, Q.; Yang, Z.; Song, Y.; Zhang, J.; Huang, P.; Chen, Z.; Dong, Y.; Fang, W.; Yi, X. Electrochemically Driven Formation of Sponge-Like Porous Silver Nanocubes Toward Efficient CO₂ Electroreduction to CO. *ChemSusChem* **2020**. [[CrossRef](#)] [[PubMed](#)]
24. Zhang, T.; Li, X.; Qiu, Y.; Su, P.; Xu, W.; Zhong, H.; Zhang, H. Multilayered Zn nanosheets as an electrocatalyst for efficient electrochemical reduction of CO₂. *J. Catal.* **2018**, *357*, 154–162. [[CrossRef](#)]
25. Zhu, W.; Zhang, L.; Yang, P.; Hu, C.; Luo, Z.; Chang, X.; Zhao, Z.J.; Gong, J. Low-Coordinated Edge Sites on Ultrathin Palladium Nanosheets Boost Carbon Dioxide Electroreduction Performance. *Angew. Chem.* **2018**, *130*, 11718–11722. [[CrossRef](#)]
26. Lai, Q.; Yuan, W.; Huang, W.; Yuan, G. Sn/SnO_x electrode catalyst with mesoporous structure for efficient electroreduction of CO₂ to formate. *Appl. Surf. Sci.* **2020**, *508*, 145221. [[CrossRef](#)]
27. Fan, M.; Garbarino, S.; Botton, G.A.; Tavares, A.C.; Guay, D. Selective electroreduction of CO₂ to formate on 3D [100] Pb dendrites with nanometer-sized needle-like tips. *J. Mater. Chem. A* **2017**, *5*, 20747–20756. [[CrossRef](#)]
28. Shao, L.; Lv, W.; Zhang, R.; Kong, F.; Cheng, L.; Wang, W. A highly efficient bi-based electrocatalyst for the reduction of CO₂ to formate. *Int. J. Electrochem. Sci.* **2019**, *14*, 114–125. [[CrossRef](#)]
29. Luo, W.; Xie, W.; Li, M.; Zhang, J.; Züttel, A. 3D hierarchical porous indium catalyst for highly efficient electroreduction of CO₂. *J. Mater. Chem. A* **2019**, *7*, 4505–4515. [[CrossRef](#)]
30. Larrazábal, G.O.; Martín, A.J.; Pérez-Ramírez, J. Building Blocks for High Performance in Electrocatalytic CO₂ Reduction: Materials, Optimization Strategies, and Device Engineering. *J. Phys. Chem. Lett.* **2017**, *8*, 3933–3944. [[CrossRef](#)] [[PubMed](#)]
31. Bagger, A.; Ju, W.; Varela, A.S.; Strasser, P.; Rossmeisl, J. Electrochemical CO₂ Reduction: A Classification Problem. *ChemPhysChem* **2017**, *18*, 3266–3273. [[CrossRef](#)]
32. Wu, J.; Huang, Y.; Ye, W.; Li, Y. CO₂ Reduction: From the Electrochemical to Photochemical Approach. *Adv. Sci.* **2017**, *4*, 1700194. [[CrossRef](#)]
33. Long, C.; Li, X.; Guo, J.; Shi, Y.; Liu, S.; Tang, Z. Electrochemical Reduction of CO₂ over Heterogeneous Catalysts in Aqueous Solution: Recent Progress and Perspectives. *Small Methods* **2018**, *3*, 1800369. [[CrossRef](#)]
34. Gao, D.; Zegkinoglou, I.; Divins, N.J.; Scholten, F.; Sinev, I.; Grosse, P.; Cuenya, B.R. Plasma-Activated Copper Nanocube Catalysts for Efficient Carbon Dioxide Electroreduction to Hydrocarbons and Alcohols. *ACS Nano* **2017**, *11*, 4825–4831. [[CrossRef](#)]

35. Grosse, P.; Gao, D.; Scholten, F.; Sinev, I.; Mistry, H.; Cuenya, B.R. Dynamic Changes in the Structure, Chemical State and Catalytic Selectivity of Cu Nanocubes during CO₂ Electroreduction: Size and Support Effects. *Angew. Chem. Int. Ed.* **2018**, *57*, 6192–6197. [[CrossRef](#)]
36. Liu, S.; Huang, S. Size effects and active sites of Cu nanoparticle catalysts for CO₂ electroreduction. *Appl. Surf. Sci.* **2019**, *475*, 20–27. [[CrossRef](#)]
37. Merino-Garcia, I.; Albo, J.; Irabien, A. Tailoring gas-phase CO₂ electroreduction selectivity to hydrocarbons at Cu nanoparticles. *Nanotechnology* **2017**, *29*, 1–16. [[CrossRef](#)] [[PubMed](#)]
38. Vennekoetter, J.B.; Sengpiel, R.; Wessling, M. Beyond the catalyst: How electrode and reactor design determine the product spectrum during electrochemical CO₂ reduction. *Chem. Eng. J.* **2019**, *364*, 89–101. [[CrossRef](#)]
39. Díaz-Sainz, G.; Alvarez-Guerra, M.; Irabien, A. Continuous Electrochemical Reduction of CO₂ to Formate: Comparative Study of the Influence of the Electrode Configuration with Sn and Bi-Based Electrocatalysts. *Molecules* **2020**, *25*, 4457. [[CrossRef](#)] [[PubMed](#)]
40. Luo, W.; Zhang, J.; Li, M.; Züttel, A. Boosting CO Production in Electrocatalytic CO₂ Reduction on Highly Porous Zn Catalysts. *ACS Catal.* **2019**, *9*, 3783–3791. [[CrossRef](#)]
41. Duan, X.; Xu, J.; Wei, Z.; Ma, J.; Guo, S.; Wang, S.; Liu, H.; Dou, S. Metal-Free Carbon Materials for CO₂ Electrochemical Reduction. *Adv. Mater.* **2017**, *29*, 1701784. [[CrossRef](#)]
42. Cui, H.; Guo, Y.; Guo, L.; Wang, L.; Zhou, Z.; Peng, Z. Heteroatom-doped carbon materials and their composites as electrocatalysts for CO₂ reduction. *J. Mater. Chem. A* **2018**, *6*, 18782–18793. [[CrossRef](#)]
43. Liu, X.; Dai, L. Carbon-based metal-free catalysts. *Nat. Rev. Mater.* **2016**, *1*. [[CrossRef](#)]
44. Sangiorgi, N.; Tuci, G.; Sanson, A.; Peruzzini, M.; Giambastiani, G. Metal-free carbon-based materials for electrocatalytic and photo-electrocatalytic CO₂ reduction. *Rend. Lincei* **2019**, *30*, 497–513. [[CrossRef](#)]
45. Li, L.; Huang, Y.; Li, Y. Carbonaceous materials for electrochemical CO₂ reduction. *EnergyChem* **2020**, *2*, 100024. [[CrossRef](#)]
46. Wu, J.; Sharifi, T.; Gao, Y.; Zhang, T.; Ajayan, P.M. Emerging Carbon-Based Heterogeneous Catalysts for Electrochemical Reduction of Carbon Dioxide into Value-Added Chemicals. *Adv. Mater.* **2019**. [[CrossRef](#)] [[PubMed](#)]
47. Jia, C.; Dastafkan, K.; Ren, W.; Yang, W.; Zhao, C. Carbon-based catalysts for electrochemical CO₂ reduction. *Sustain. Energy Fuels* **2019**. [[CrossRef](#)]
48. Liu, S.; Yang, H.; Su, X.; Ding, J.; Mao, Q.; Huang, Y.; Zhang, T.; Liu, B. Rational design of carbon-based metal-free catalysts for electrochemical carbon dioxide reduction: A review. *J. Energy Chem.* **2019**. [[CrossRef](#)]
49. Fernandes, D.M.; Peixoto, A.F.; Freire, C. Nitrogen-doped metal-free carbon catalysts for (electro)chemical CO₂ conversion and valorisation. *Dalton Trans.* **2019**, *48*, 13508–13528. [[CrossRef](#)]
50. Wang, H.; Chen, Y.; Hou, X.; Ma, C.; Tan, T. Nitrogen-doped graphenes as efficient electrocatalysts for the selective reduction of carbon dioxide to formate in aqueous solution. *Green Chem.* **2016**, *18*, 3250–3256. [[CrossRef](#)]
51. Sun, X.; Kang, X.; Zhu, Q.; Ma, J.; Yang, G.; Liu, Z.; Han, B. Very highly efficient reduction of CO₂ to CH₄ using metal-free N-doped carbon electrodes. *Chem. Sci.* **2016**, *7*, 2883–2887. [[CrossRef](#)]
52. Yuan, J.; Zhi, W.Y.; Liu, L.; Yang, M.P.; Wang, H.; Lu, J.X. Electrochemical reduction of CO₂ at metal-free N-functionalized graphene oxide electrodes. *Electrochim. Acta* **2018**, *282*, 694–701. [[CrossRef](#)]
53. Liu, S.; Yang, H.; Huang, X.; Liu, L.; Cai, W.; Gao, J.; Li, X.; Zhang, T.; Huang, Y.; Liu, B. Identifying Active Sites of Nitrogen-Doped Carbon Materials for the CO₂ Reduction Reaction. *Adv. Funct. Mater.* **2018**, *28*, 1800499. [[CrossRef](#)]
54. Wu, J.; Ma, S.; Sun, J.; Gold, J.I.; Tiwary, C.; Kim, B.; Zhu, L.; Chopra, N.; Odeh, I.N.; Vajtai, R.; et al. A metal-free electrocatalyst for carbon dioxide reduction to multi-carbon hydrocarbons and oxygenates. *Nat. Commun.* **2016**, *7*, 13869. [[CrossRef](#)]
55. Verma, S.; Nwabara, U.O.; Kenis, P.J.A. *Carbon-Based Electrodes and Catalysts for the Electroreduction of Carbon Dioxide (CO₂) to Value-Added Chemicals*; Springer: Berlin/Heidelberg, Germany, 2019; ISBN 9783319929170.
56. Wu, J.; Yadav, R.M.; Liu, M.; Sharma, P.P.; Tiwary, C.S.; Ma, L.; Zou, X.; Zhou, X.; Jakobson, B.I.; Lou, J.; et al. Achieving Highly Efficient, Selective, and Stable CO₂ Reduction on Nitrogen-Doped Carbon Nanotubes. *ACS Nano* **2015**, *9*, 5364–5371. [[CrossRef](#)]

57. Xu, J.; Kan, Y.; Huang, R.; Zhang, B.; Wang, B.; Wu, K.H.; Lin, Y.; Sun, X.; Li, Q.; Centi, G.; et al. Revealing the Origin of Activity in Nitrogen-Doped Nanocarbons towards Electrocatalytic Reduction of Carbon Dioxide. *ChemSusChem* **2016**, *9*, 1085–1089. [[CrossRef](#)]
58. Ma, C.; Hou, P.; Wang, X.; Wang, Z.; Li, W.; Kang, P. Carbon nanotubes with rich pyridinic nitrogen for gas phase CO₂ electroreduction. *Appl. Catal. B Environ.* **2019**, *250*, 347–354. [[CrossRef](#)]
59. Zhou, W.; Shen, H.; Wang, Q.; Onoe, J.; Kawazoe, Y.; Jena, P. N-doped peanut-shaped carbon nanotubes for efficient CO₂ electrocatalytic reduction. *Carbon N. Y.* **2019**, *152*, 241–246. [[CrossRef](#)]
60. Zheng, Y.; Cheng, P.; Xu, J.; Han, J.; Wang, D.; Hao, C.; Alanagh, H.R.; Long, C.; Shi, X.; Tang, Z. MOF-derived nitrogen-doped nanoporous carbon for electroreduction of CO₂ to CO: The calcining temperature effect and the mechanism. *Nanoscale* **2019**, *11*, 4911–4917. [[CrossRef](#)] [[PubMed](#)]
61. Zhong, X.; Zhong, H.; Jin, F. Zeolitic imidazolate frameworks derived nitrogen doped porous carbon for electrochemical reduction of CO₂. *IOP Conf. Ser. Earth Environ. Sci.* **2020**, *450*. [[CrossRef](#)]
62. Chen, Z.; Mou, K.; Yao, S.; Liu, L. Highly selective electrochemical reduction of CO₂ to formate on metal-free nitrogen-doped PC61BM. *J. Mater. Chem. A* **2018**, *6*, 11236–11243. [[CrossRef](#)]
63. Sun, Z.; Li, K.; Koh, S.W.; Jiao, L. Low-Cost and Scalable Fabrication of Hierarchically Porous N-Doped Carbon for Energy Storage and Conversion Application. *ChemistrySelect* **2020**, *5*, 533–537. [[CrossRef](#)]
64. Liu, Y.; Chen, S.; Quan, X.; Yu, H. Efficient Electrochemical Reduction of Carbon Dioxide to Acetate on Nitrogen-Doped Nanodiamond. *J. Am. Chem. Soc.* **2015**, *137*, 11631–11636. [[CrossRef](#)]
65. Salinas-Torres, D.; Navlani-García, M.; Mori, K.; Kuwahara, Y.; Yamashita, H. Nitrogen-doped carbon materials as a promising platform toward the efficient catalysis for hydrogen generation. *Appl. Catal. A Gen.* **2019**, *571*, 25–41. [[CrossRef](#)]
66. Liu, T.; Ali, S.; Lian, Z.; Li, B.; Su, D.S. CO₂ electroreduction reaction on heteroatom-doped carbon cathode materials. *J. Mater. Chem. A* **2017**, *5*, 21596–21603. [[CrossRef](#)]
67. Li, C.; Wang, Y.; Xiao, N.; Li, H.; Ji, Y.; Guo, Z.; Liu, C.; Qiu, J. Nitrogen-doped porous carbon from coal for high efficiency CO₂ electrocatalytic reduction. *Carbon N. Y.* **2019**, *151*, 46–52. [[CrossRef](#)]
68. Xu, J.; Zhang, B.; Wang, B.; Wu, K.H.; Peng, Z.; Li, Q.; Centi, G.; Su, D.S. Decisive Intermediates Responsible for the Carbonaceous Products of CO₂ Electro-reduction on Nitrogen-Doped sp² Nanocarbon Catalysts in NaHCO₃ Aqueous Electrolyte. *ChemElectroChem* **2017**, *4*, 1274–1278. [[CrossRef](#)]
69. Li, H.; Xiao, N.; Wang, Y.; Li, C.; Ye, X.; Guo, Z.; Pan, X.; Liu, C.; Bai, J.; Xiao, J.; et al. Nitrogen-doped tubular carbon foam electrodes for efficient electroreduction of CO₂ to syngas with potential-independent CO/H₂ ratios. *J. Mater. Chem. A* **2019**, *7*, 18852–18860. [[CrossRef](#)]
70. Kuang, M.; Guan, A.; Gu, Z.; Han, P.; Qian, L.; Zheng, G. Enhanced N-doping in mesoporous carbon for efficient electrocatalytic CO₂ conversion. *Nano Res.* **2019**, *12*, 2324–2329. [[CrossRef](#)]
71. Wang, H.; Jia, J.; Song, P.; Wang, Q.; Li, D.; Min, S.; Qian, C.; Wang, L.; Li, Y.F.; Ma, C.; et al. Efficient Electrocatalytic Reduction of CO₂ by Nitrogen-Doped Nanoporous Carbon/Carbon Nanotube Membranes: A Step Towards the Electrochemical CO₂ Refinery. *Angew. Chem. Int. Ed.* **2017**, *56*, 7847–7852. [[CrossRef](#)]
72. Saravanan, K.; Gottlieb, E.; Keith, J.A. Nitrogen-doped nanocarbon materials under electroreduction operating conditions and implications for electrocatalysis of CO₂. *Carbon N. Y.* **2017**, *111*, 859–866. [[CrossRef](#)]
73. Siahrostami, S.; Jiang, K.; Karamad, M.; Chan, K.; Wang, H.; Nørskov, J. Theoretical Investigations into Defected Graphene for Electrochemical Reduction of CO₂. *ACS Sustain. Chem. Eng.* **2017**, *5*, 11080–11085. [[CrossRef](#)]
74. Silva, W.O.; Silva, G.C.; Webster, R.F.; Benedetti, T.M.; Tilley, R.D.; Ticianelli, E.A. Electrochemical Reduction of CO₂ on Nitrogen-Doped Carbon Catalysts With and Without Iron. *ChemElectroChem* **2019**, *6*, 4626–4636. [[CrossRef](#)]
75. Liu, Y.; Zhao, J.; Cai, Q. Pyrrolic-nitrogen doped graphene: A metal-free electrocatalyst with high efficiency and selectivity for the reduction of carbon dioxide to formic acid: A computational study. *Phys. Chem. Chem. Phys.* **2016**, *18*, 5491–5498. [[CrossRef](#)]
76. Ma, T.; Fan, Q.; Tao, H.; Han, Z.; Jia, M.; Gao, Y.; Ma, W.; Sun, Z. Heterogeneous electrochemical CO₂ reduction using nonmetallic carbon-based catalysts: Current status and future challenges. *Nanotechnology* **2017**, *28*, 472001. [[CrossRef](#)]
77. Song, Y.; Chen, W.; Zhao, C.; Li, S.; Wei, W.; Sun, Y. Metal-Free Nitrogen-Doped Mesoporous Carbon for Electroreduction of CO₂ to Ethanol. *Angew. Chem. Int. Ed.* **2017**, *56*, 10840–10844. [[CrossRef](#)] [[PubMed](#)]

78. Wang, W.; Shang, L.; Chang, G.; Yan, C.; Shi, R.; Zhao, Y.; Waterhouse, G.I.N.; Yang, D.; Zhang, T. Intrinsic Carbon-Defect-Driven Electrocatalytic Reduction of Carbon Dioxide. *Adv. Mater.* **2019**, *31*, 1808276. [[CrossRef](#)] [[PubMed](#)]
79. Wanninayake, N.; Ai, Q.; Zhou, R.; Hoque, M.A.; Herrell, S.; Guzman, M.I.; Risko, C.; Kim, D.Y. Understanding the effect of host structure of nitrogen doped ultrananocrystalline diamond electrode on electrochemical carbon dioxide reduction. *Carbon N. Y.* **2020**, *157*, 408–419. [[CrossRef](#)]
80. Hursán, D.; Samu, A.A.; Janovák, L.; Artyushkova, K.; Asset, T.; Atanassov, P.; Janáky, C. Morphological Attributes Govern Carbon Dioxide Reduction on N-Doped Carbon Electrodes. *Joule* **2019**, *3*, 1719–1733. [[CrossRef](#)]
81. Zhang, H.; Min, S.; Wang, F.; Zhang, Z.; Kong, C. Efficient electrocatalytic CO₂ reduction to CO with high selectivity using a N-doped carbonized wood membrane. *New J. Chem.* **2020**. [[CrossRef](#)]
82. Zhu, Y.; Lv, K.; Wang, X.; Yang, H.; Xiao, G.; Zhu, Y. 1D/2D nitrogen-doped carbon nanorod arrays/ultrathin carbon nanosheets: Outstanding catalysts for the highly efficient electroreduction of CO₂ to CO. *J. Mater. Chem. A* **2019**, *7*, 14895–14903. [[CrossRef](#)]
83. Chen, C.; Sun, X.; Yan, X.; Wu, Y.; Liu, H.; Zhu, Q.; Bediako, B.B.A.; Han, B. Boosting CO₂ electroreduction on N, P-co-doped carbon aerogels. *Angew. Chem.* **2020**. [[CrossRef](#)]
84. Ikemiya, N.; Natsui, K.; Nakata, K.; Einaga, Y. Effect of alkali-metal cations on the electrochemical reduction of carbon dioxide to formic acid using boron-doped diamond electrodes. *RSC Adv.* **2017**, *7*, 22510–22514. [[CrossRef](#)]
85. Ikemiya, N.; Natsui, K.; Nakata, K.; Einaga, Y. Long-Term Continuous Conversion of CO₂ to Formic Acid Using Boron-Doped Diamond Electrodes. *ACS Sustain. Chem. Eng.* **2018**, *6*, 8108–8112. [[CrossRef](#)]
86. Tomisaki, M.; Natsui, K.; Ikemiya, N.; Nakata, K.; Einaga, Y. Influence of Electrolyte on the Electrochemical Reduction of Carbon Dioxide Using Boron-Doped Diamond Electrodes. *ChemistrySelect* **2018**, *3*, 10209–10213. [[CrossRef](#)]
87. Jiwanti, P.K.; Natsui, K.; Nakata, K.; Einaga, Y. Selective production of methanol by the electrochemical reduction of CO₂ on boron-doped diamond electrodes in aqueous ammonia solution. *RSC Adv.* **2016**, *6*, 102214–102217. [[CrossRef](#)]
88. Liu, Y.; Zhang, Y.; Cheng, K.; Quan, X.; Fan, X.; Su, Y.; Chen, S.; Zhao, H.; Zhang, Y.; Yu, H.; et al. Selective Electrochemical Reduction of Carbon Dioxide to Ethanol on a Boron- and Nitrogen-Co-doped Nanodiamond. *Angew. Chem. Int. Ed.* **2017**, *56*, 15607–15611. [[CrossRef](#)] [[PubMed](#)]
89. Jia, C.; Ren, W.; Chen, X.; Yang, W.; Zhao, C. (N, B) Dual Heteroatom-Doped Hierarchical Porous Carbon Framework for Efficient Electroreduction of Carbon Dioxide. *ACS Sustain. Chem. Eng.* **2020**, *8*, 6003–6010. [[CrossRef](#)]
90. Sreekanth, N.; Nazrulla, M.A.; Vineesh, T.V.; Sailaja, K.; Phani, K.L. Metal-free boron-doped graphene for selective electroreduction of carbon dioxide to formic acid/formate. *Chem. Commun.* **2015**, *51*, 16061–16064. [[CrossRef](#)] [[PubMed](#)]
91. Kumik, A.; Ivandini, T.A.; Wibowo, R. Modification of boron-doped diamond with gold-palladium nanoparticles for CO₂ electroreduction. *IOP Conf. Ser. Mater. Sci. Eng.* **2020**, *763*. [[CrossRef](#)]
92. Saprudin, M.H.; Atriardi, S.R.; Gunlazuardi, J.; Einaga, Y.; Ivandini, T.A. Electroreduction of carbon dioxide using platinum-iridium modified boron-doped diamond (BDD) with various platinum-iridium ratios. *IOP Conf. Ser. Mater. Sci. Eng.* **2020**, *763*, 012051. [[CrossRef](#)]
93. Denala, D.; Khalil, M.; Ivandini, T.A. Preparation of boron doped diamond modified with cuprous oxide as working electrode for electroreduction of CO₂. *AIP Conf. Proc.* **2019**, *2168*, 020057.
94. Dewandaru, R.K.P.; Gunlazuardi, J.; Ivandini, T.A. Preparation of iridium-modified boron-doped diamond (BDD) electrodes for electroreduction of CO₂. *AIP Conf. Proc.* **2018**, *2023*, 020098. [[CrossRef](#)]
95. Ivandini, T.A. Electrochemical conversion of CO₂ at metal-modified boron-doped diamond electrodes. *AIP Conf. Proc.* **2018**, *2023*, 020102. [[CrossRef](#)]
96. Jasril Gunlazuardi, J.; Ivandini, T.A. Preparation of platinum-modified boron-doped diamond for electroreduction of CO₂. *IOP Conf. Ser. Mater. Sci. Eng.* **2017**, *188*, 012037. [[CrossRef](#)]
97. Jiwanti, P.K.; Ichzan, A.M.; Dewandaru, R.K.P.; Atriardi, S.R.; Einaga, Y.; Ivandini, T.A. Improving the CO₂ electrochemical reduction to formic acid using iridium-oxide-modified boron-doped diamond electrodes. *Diam. Relat. Mater.* **2020**, *106*, 107874. [[CrossRef](#)]

98. Jiwanti, P.K.; Aritonang, R.P.; Abdullah, I.; Einaga, Y.; Ivandini, T.A. Copper-nickel-modified Boron-doped Diamond Electrode for CO₂ Electrochemical Reduction Application: A Preliminary Study. *IOP Conf. Ser. Mater. Sci. Eng.* **2019**, *23*, 204–209. [[CrossRef](#)]
99. Ichzan, A.M.; Gunlazuardi, J.; Ivandini, T.A. Preparation of boron doped diamond modified by iridium for electroreduction of carbon dioxide (CO₂). *IOP Conf. Ser. Mater. Sci. Eng.* **2017**, *188*, 012030. [[CrossRef](#)]
100. Yetri, N.Y.; Ivandini, T.A.; Gunlazuardi, J. Preparation of copper oxide modified boron-doped diamond electrodes and its preliminary study for CO₂ reduction. *IOP Conf. Ser. Mater. Sci. Eng.* **2017**, *188*, 012011. [[CrossRef](#)]
101. Jiwanti, P.K.; Natsui, K.; Einaga, Y. The Utilization of Boron-doped Diamond Electrodes for the Electrochemical Reduction of CO₂: Toward the production compounds with a high number of carbon atoms. *Electrochemistry* **2019**, *87*, 109–113. [[CrossRef](#)]
102. Natsui, K.; Iwakawa, H.; Ikemiya, N.; Nakata, K.; Einaga, Y. Stable and Highly Efficient Electrochemical Production of Formic Acid from Carbon Dioxide Using Diamond Electrodes. *Angew. Chem. Int. Ed.* **2018**, *57*, 2639–2643. [[CrossRef](#)]
103. Xu, J.; Natsui, K.; Naoi, S.; Nakata, K.; Einaga, Y. Effect of doping level on the electrochemical reduction of CO₂ on boron-doped diamond electrodes. *Diam. Relat. Mater.* **2018**, *86*, 167–172. [[CrossRef](#)]
104. Tomisaki, M.; Kasahara, S.; Natsui, K.; Ikemiya, N.; Einaga, Y. Switchable Product Selectivity in the Electrochemical Reduction of Carbon Dioxide Using Boron-Doped Diamond Electrodes. *J. Am. Chem. Soc.* **2019**, *141*, 7414–7420. [[CrossRef](#)]
105. Luo, D.; Liu, S.; Nakata, K.; Fujishima, A. Electrochemical reduction of CO₂ and degradation of KHP on boron-doped diamond electrodes in a simultaneous and enhanced process. *Chin. Chem. Lett.* **2019**, *30*, 509–512. [[CrossRef](#)]
106. Zhao, J.; Chen, Z.; Zhao, J. Metal-free graphdiyne doped with sp-hybridized boron and nitrogen atoms at acetylenic sites for high-efficiency electroreduction of CO₂ to CH₄ and C₂H₄. *J. Mater. Chem. A* **2019**, *7*, 4026–4035. [[CrossRef](#)]
107. Mou, S.; Wu, T.; Xie, J.; Zhang, Y.; Ji, L.; Huang, H.; Wang, T.; Luo, Y.; Xiong, X.; Tang, B.; et al. Boron Phosphide Nanoparticles: A Nonmetal Catalyst for High-Selectivity Electrochemical Reduction of CO₂ to CH₃OH. *Adv. Mater.* **2019**, *31*, 1903499. [[CrossRef](#)] [[PubMed](#)]
108. Wang, F.; Song, S.; Li, K.; Li, J.; Pan, J.; Yao, S.; Ge, X.; Feng, J.; Wang, X.; Zhang, H. A “Solid Dual-Ions-Transformation” Route to S,N Co-Doped Carbon Nanotubes as Highly Efficient “Metal-Free” Catalysts for Organic Reactions. *Adv. Mater.* **2016**, *28*, 10679–10683. [[CrossRef](#)] [[PubMed](#)]
109. Li, W.; Seredych, M.; Rodríguez-Castellón, E.; Bandoz, T.J. Metal-free Nanoporous Carbon as a Catalyst for Electrochemical Reduction of CO₂ to CO and CH₄. *ChemSusChem* **2016**, *9*, 606–616. [[CrossRef](#)] [[PubMed](#)]
110. Pan, F.; Li, B.; Deng, W.; Du, Z.; Gang, Y.; Wang, G.; Li, Y. Promoting electrocatalytic CO₂ reduction on nitrogen-doped carbon with sulfur addition. *Appl. Catal. B Environ.* **2019**, *252*, 240–249. [[CrossRef](#)]
111. Yang, H.; Wu, Y.; Lin, Q.; Fan, L.; Chai, X.; Zhang, Q.; Liu, J.; He, C.; Lin, Z. Composition Tailoring via N and S Co-doping and Structure Tuning by Constructing Hierarchical Pores: Metal-Free Catalysts for High-Performance Electrochemical Reduction of CO₂. *Angew. Chem.* **2018**, *130*, 15702–15706. [[CrossRef](#)]
112. Li, G.; Qin, Y.; Wu, Y.; Pei, L.; Hu, Q.; Yang, H.; Zhang, Q.; Liu, J.; He, C. Nitrogen and sulfur dual-doped high-surface-area hollow carbon nanospheres for efficient CO₂ reduction. *Chin. J. Catal.* **2020**, *41*, 830–838. [[CrossRef](#)]
113. Han, H.; Park, S.; Jang, D.; Lee, S.; Kim, W.B. Electrochemical Reduction of CO₂ to CO by N,S Dual-Doped Carbon Nanoweb Catalysts. *ChemSusChem* **2020**, *13*, 539–547. [[CrossRef](#)]
114. Wang, G.; Liu, M.; Jia, J.; Xu, H.; Zhao, B.; Lai, K.; Tu, C.; Wen, Z. Nitrogen and Sulfur Co-doped Carbon Nanosheets for Electrochemical Reduction of CO₂. *ChemCatChem* **2020**, *12*, 2203–2208. [[CrossRef](#)]
115. Xie, J.; Zhao, X.; Wu, M.; Li, Q.; Wang, Y.; Yao, J. Metal-Free Fluorine-Doped Carbon Electrocatalyst for CO₂ Reduction Outcompeting Hydrogen Evolution. *Angew. Chem.* **2018**, *130*, 9788–9792. [[CrossRef](#)]
116. Ni, W.; Xue, Y.; Zang, X.; Li, C.; Wang, H.; Yang, Z.; Yan, Y.M. Fluorine Doped Cage-like Carbon Electrocatalyst: An Insight into the Structure-Enhanced CO Selectivity for CO₂ Reduction at High Overpotential. *ACS Nano* **2020**, *14*, 2014–2023. [[CrossRef](#)]
117. Panomsuwan, G.; Saito, N.; Ishizaki, T. Simple one-step synthesis of fluorine-doped carbon nanoparticles as potential alternative metal-free electrocatalysts for oxygen reduction reaction. *J. Mater. Chem. A* **2015**, *3*, 9972–9981. [[CrossRef](#)]

118. Zaderko, A.N.; Horodetska, D.S.; Grishchenko, L.M.; Diyuk, V.E.; Boldyrieva, O.Y.; Lisnyak, V.V.; Novychenko, N.S.; Skryshevsky, V.A.; Khomenko, V.G. Fluororganic Groups Grafted on Carbon Microspheres. In Proceedings of the 2019 IEEE 9th International Conference on Nanomaterials: Applications and Properties, NAP 2019, Odesa, Ukraine, 15–20 September 2019; pp. 15–20.
119. Pu, L.; Ma, Y.; Zhang, W.; Hu, H.; Zhou, Y.; Wang, Q.; Pei, C. Simple method for the fluorinated functionalization of graphene oxide. *RSC Adv.* **2013**, *3*, 3881–3884. [[CrossRef](#)]
120. Wang, Y.; Chen, J.; Wang, G.; Li, Y.; Wen, Z. Perfluorinated Covalent Triazine Framework Derived Hybrids for the Highly Selective Electroconversion of Carbon Dioxide into Methane. *Angew. Chem. Int. Ed.* **2018**, *57*, 13120–13124. [[CrossRef](#)] [[PubMed](#)]
121. Pan, F.; Li, B.; Xiang, X.; Wang, G.; Li, Y. Efficient CO₂ Electroreduction by Highly Dense and Active Pyridinic Nitrogen on Holey Carbon Layers with Fluorine Engineering. *ACS Catal.* **2019**, *9*, 2124–2133. [[CrossRef](#)]

Publisher's Note: MDPI stays neutral with regard to jurisdictional claims in published maps and institutional affiliations.



© 2020 by the authors. Licensee MDPI, Basel, Switzerland. This article is an open access article distributed under the terms and conditions of the Creative Commons Attribution (CC BY) license (<http://creativecommons.org/licenses/by/4.0/>).